Available online at www.sciencedirect.com
SCIENCE DIRECT®
Journal of Power Sources 133 (2004) 320–328
JOURNAL OF POWER SOURCES
www.elsevier.com/locate/jpowsour

Influence of the solvent properties on the characteristics of a double layer capacitor

M. Arulepp[a,b,*], L. Permann[a,b], J. Leis[a,c], A. Perkson[a], K. Rumma[a], A. Jänes[a,b], E. Lust[b]

[a] *Tartu Technologies Ltd., 185 Riia Str., 51014 Tartu, Estonia*
[b] *Institute of Physical Chemistry, University of Tartu, 2 Jakobi Str., 51014 Tartu, Estonia*
[c] *Institute of Chemical Physics, University of Tartu, 2 Jakobi Str., 51014 Tartu, Estonia*

Received 10 November 2003; received in revised form 4 March 2004; accepted 8 March 2004

Abstract

Electrochemical and electrical double layer characteristics for the phase boundary nanoporous carbon |1.0 M triethylmethylammonium tetrafluoroborate (TEMA) solution in acetonitrile (AN), γ-butyrolactone (GBL), acetone (DMK) and propylene carbonate (PC) have been studied using the cyclic voltammetry (CV) and the electrochemical impedance spectroscopy (EIS) methods. The constant current and constant power charge/discharge characteristics of capacitor modules constructed and filled with different electrolytes were tested over the temperature range from −30 to +60 °C. Tests for "lifetime" of the capacitors were performed at elevated temperature. Energy density versus power density, i.e. so-called Ragone plots were constructed to characterize the performance of the capacitor modules. It was established that the energy density, power density, discharge time, etc. of the electrical double layer capacitors (EDLC) depend on the pore size distribution and conductivity of the nanoporous electrode material. It was shown that the energy output of capacitor depends on the viscosity and molar conductivity of a solvent. The power output of the capacitor increased in the order of solvent PC < DMK < GBL < AN in agreement with the dependence of the Ragone plot parameters on temperature.

Keywords: Nanoporous carbon; Nonaqueous electrolyte solution; Double layer capacitor

1. Theoretical background

Electrical double layer capacitors (EDLC) (supercapacitors) are the intermediate systems between electrochemical batteries that can store high energy density associated with low power density values, and dielectric capacitors, which can deliver very high power during few milliseconds [1]. Supercapacitors can generate high specific power during few seconds or more, which leads to the specific energy densities ranging from 0.5 to 10 Wh kg^{-1}. There are three different types of supercapacitors based on the different electrode materials and working principles: (1) carbon/carbon, (2) metal oxide and (3) electronically conducting polymers. This work is focused on carbon/carbon supercapacitors [1].

The important advantages of carbon/carbon EDLC are their very good reversibility and the comparatively low temperature coefficient. As the electrostatic interactions are significantly less detrimental to electrodes and solution stability than the usual electrochemical redox reactions, used for the generation of electricity in the fuel cells and various batteries, EDLC can be recharged–discharged up to 10^6 times [1]. It is well known that the performance characteristics of an EDLC, e.g. in terms of the relations between achieved power densities and corresponding energy densities depend on the equivalent series resistance (ESR) and the internal distribution of electrode resistance (IER) in the pore matrix of the electrodes [1–17].

The capacitance of EDLC depends mainly on the carbon material used for preparation of the electrodes. Theoretically, the higher is the surface area of the activated carbon, the higher specific capacitance should be expected. However, the practical situation is more complicated and usually the capacitance measured does not have the linear relationship with the specific surface area of the electrode material. The main reason for this phenomenon is that the nanopores with small diameter may not be accessible to the electrolyte

* Corresponding author. Tel.: +372-7-383-057; fax: +372-7-428-467.
E-mail address: matia@park.tartu.ee (M. Arulepp).

0378-7753/$ – see front matter © 2004 Elsevier B.V. All rights reserved.
doi:10.1016/j.jpowsour.2004.03.026

solution simply because the electrolyte ions, especially big organic ions and ions with the solvation cell, are too big to enter into the nanopores. Thus, the surface area of these non-accessible nanopores will not contribute to the total double layer capacitance of the electrode material.

The most frequently employed methods for testing of the EDL capacitors are (1) the cyclic voltammetry (CV) for generating the charge–discharge curves; (2) galvanostatic methods such as, e.g. current step, and constant current methods (CC) at I = constant; (3) constant power method at P = constant (CP); (4) the electrochemical impedance spectroscopy (EIS).

1.1. Cyclic voltammetry

In the case of CV applied at a cell potential sweep-rate $v = \pm \mathrm{d}U/\mathrm{d}t$ ($\mathrm{V\,s^{-1}}$), the current response of a capacitor with the capacitance C is given as

$$i = C\frac{\mathrm{d}U}{\mathrm{d}t} = Cv \tag{1}$$

Quite often, for carbon double layer capacitors, Faradaic pseudocapacitance devices and hybrid devices C is a function of cell potential U during charge or discharge cycle, i.e. $C(U) \equiv f(U)$. Then

$$i = C(U)\frac{\mathrm{d}U}{\mathrm{d}t} = C(U)v \tag{2}$$

Thus, from Eqs. (1) and (2) $C(U)$ is directly obtainable as $i(U)/v$, where $i(U)$ is a potential and potential sweep rate dependent current density. It should be noted that by CV at moderate scan-rates a differential capacitance $C = \mathrm{d}q/\mathrm{d}U$ is directly generated rather than the integral capacitance $\bar{C} = \Delta q/\Delta U$. The integral between potentials U_1 and U_2, in CV gives directly the charge Δq, passed between these two potentials:

$$\Delta q = \int_{U_1}^{U_2} C(U)\frac{\mathrm{d}U}{\mathrm{d}t}\mathrm{d}t = \int_{U_1}^{U_2} C(U)\,\mathrm{d}U \tag{3}$$

1.2. Electrochemical impedance spectroscopy

Electrochemical impedance spectroscopy is based on a modulation function $U(t) = V_0 \sin \omega t$, where $\omega = 2\pi f$ is the angular frequency and f the ac frequency ($0.01\,\mathrm{Hz} < f < 100\,\mathrm{kHz}$). The current response of the electrical double layer (approximated as a capacitor and resistor in series) is given as

$$i(t) = C\frac{\mathrm{d}U(t)}{\mathrm{d}t} = C\omega_0 V_0 \sin(\omega t + \varphi) \tag{4}$$

where φ is a phase-shift that equals to 90° for the ideal capacitor and V_0 the alternating voltage signal amplitude. For electrochemical systems usually $\varphi \leq 90°$, depending on the presence of any effective or equivalent series resistance or on any slowness of polarization of the dielectric material of the capacitor. In electrochemical double layer capacitors the polarization slowness arises from the dipole orientation of the solvent molecules and/or from the ion adsorption, but it is observable only at higher frequencies [1–3].

The response function in EIS for an ideal capacitor can be simply represented by imaginary part of the impedance Z'', given as

$$Z'' = \frac{1}{\mathrm{j}\omega C} = -\frac{\mathrm{j}}{\omega C} \tag{5}$$

In real EDLC systems, Z'' is normally coupled with an ohmic resistance R that is either an actual or an ESR and corresponding impedance is simply written as

$$Z' \equiv R \tag{6}$$

Thus, for a real EDL capacitor (series circuit)

$$Z = Z' + Z'' = R + \frac{1}{\mathrm{j}\omega C} \tag{7}$$

from which R and C can be determined by frequency-response analysis in well-known ways [1–3].

For the real electrochemical double layer capacitor, both R and C are quantities which are distributed over a range of the effective values due to the electrode porosity, i.e. nanoporous structure of the electrode, electrolyte, EDLC separator parameter, design, etc. and the impedance Z as a function of ac frequency is a more complicated parameter than that in Eq. (7). According to de Levie [8,10,11] and Salitra et al. [5] the real system has a spectrum of "RC" time-constants and a corresponding "power spectrum". The complex impedance plane-diagram, i.e. the $-Z''$ versus Z' dependence over a range of frequencies consists mainly of two principal regions: one at 45° line at high frequencies, extrapolating to an intercept on the Z'-axis equal to the exterior solution + constant resistances; the other − a transition at a "knee" in the curve to a vertical line (ideal capacitor) for which $-Z''$ is simply $\mathrm{j}/\omega C$ at sufficiently low frequencies. The extrapolation of this line to the Z'-axis gives the total distributed and external resistance values. The so-called pore resistance R_{pore} is defined as the real component of the impedance when $\omega \to 0$.

1.3. Constant current study

In the current step technique a constant current I is applied on the cell and the potential response is measured. For a capacitive system with an ohmic resistance the potential drop ΔU at very short times τ can be expressed as

$$\Delta U = IR \tag{8}$$

In the constant current study (CC) on charging curve (U, t-curve at I = constant) Δq is directly determinable from the record of $U(t)$ versus t, i.e. $U(t)$ versus q. The capacitance of the electrode material, as well as the cell can be evaluated from the slope of the discharge curves according to the formula below:

$$C = I\frac{\mathrm{d}t}{\mathrm{d}U} \tag{9}$$

When for simplicity the charging curve is approximated by a linear function in the region dU, the medium integral capacitance values can be obtained as

$$\bar{C} = I\frac{\Delta t}{\Delta U} \tag{10}$$

From the CC curves the internal resistance can be evaluated from IR-drop after the current is changed. Regularly the response time 10 ms is used, where dU_1 is the value of the voltage during 10 ms and I the current used:

$$R = \frac{\mathrm{d}U_1}{2I} \tag{11}$$

1.4. Constant power study

For double layer capacitors the peak power capability can be estimated from a constant current discharge from the rated voltage U_w to $U_\mathrm{w}/2$ according to the Ref. [1]. Thus, the average voltage for the discharge is $(3/4)U_\mathrm{w}$. At these conditions the average efficiency EF for the discharge is

$$\mathrm{EF} = 1 - I\left(\frac{R}{(3/4)U_\mathrm{w}}\right) \tag{12}$$

The current I for the discharge at an efficiency EF is defined as

$$I = \frac{(3/4)(1-\mathrm{EF})U_\mathrm{w}}{R} \tag{13}$$

and the corresponding power is expressed as

$$P = \frac{9(1-\mathrm{EF})U_\mathrm{w}}{16R} \tag{14}$$

The matched power density is expressed as

$$P_\mathrm{matched} = \frac{U_\mathrm{w}^2}{4R} \tag{15}$$

The power density (PD) of the electrical double layer capacitor can be calculated using Eq. (16):

$$\mathrm{PD} = \frac{P}{m} \tag{16}$$

where m is the weight of the capacitor.

The power density of electrical double layer capacitor for a specified efficiency is given by

$$\mathrm{PD\,(W\,kg^{-1})} = \frac{9}{16}(1-\mathrm{EF})\frac{K_2}{K_1}U_\mathrm{w}^2 \tag{17}$$

where $K_2 = C/m$ [Ah(kg cell)$^{-1}$] (when the cell capacitance is expressed in ampere hours, Ah) and $K_1 = CR$. The energy density ED is expressed as

$$\mathrm{ED\,(Wh\,kg^{-1})} = \frac{K_2 U_\mathrm{w}^2}{7200} \tag{18}$$

It should be noted that the discussion given above is valid for EDLC, regularly the constant power method has been used and the capacitor has been cycled between maximum cell potential U_w and $U_\mathrm{w}/2$ and the power densities are between 0.1 and 10 W g^{-1}.

2. Experimental

A nanoporous carbon powder was made from titanium carbide (A. C. Starck, CA grade, 1–3 μm) by a chlorinating method [18]. TiC with an average particle size of 1.3–3.0 μm was loaded into the silica rotary kiln rector and let react with a flow of chlorine gas (99.999% pure) for 4 h in a tube furnace at 950 °C. The by-product ($TiCl_4$) was led away by the stream of the excess Cl_2. After reaction the reactor was flushed with the argon (99.9995% pure) at 1000 °C for 0.5 h to remove the excess Cl_2 and residues of a gaseous by-products from carbon. During heating and cooling the reactor was flushed with a slow stream of argon. Thereafter the resulting carbon powder was moved into silica stationary bed reactor and treated with hydrogen at 800 °C for 2.5 h. During heating and cooling the reactor was flushed with a slow stream of helium (99.9995% pure). Carbonaceous polarizable electrodes from these nanoporous carbon powders were prepared as follows. The mixture of 94% (wt.) nanoporous carbon and 6% (wt.) polytetra fluoroethylene PTFE binder (Aldrich, 60% suspension in water) was rolled stepwise into the carbon film with a final thickness of 100 ± 5 μm. After drying, the raw electrode sheets were plated from one side with a thin aluminum layer (4 ± 1 μm) using the plasma activated physical vapor deposition method.

It should be noted that the carbon powders with different pore size distribution, shown in Fig. 1, were used to produce a positively and negatively charged electrodes. Methods for modification of the pore structure to achieve a better match between the pore size and the electrolyte ion size are particularly discussed in Ref. [4,15–18]. Some characteristics of these carbon powders such as specific surface area, micropore volume and area, obtained from low temperature nitrogen sorption data using ASAP 2000 (Micromeritics, Inc.) analyzer, are presented in Table 1. Single-point BET surface area has been calculated at relative pressure $P/P_0 = 0.2$ and the total pore volume at near to a saturation pressure, $P/P_0 = 0.99$. The volume and surface area of micropores were derived from the so-called t-plot dependence of nitrogen sorption isotherm using the Harkins–Jura statistical

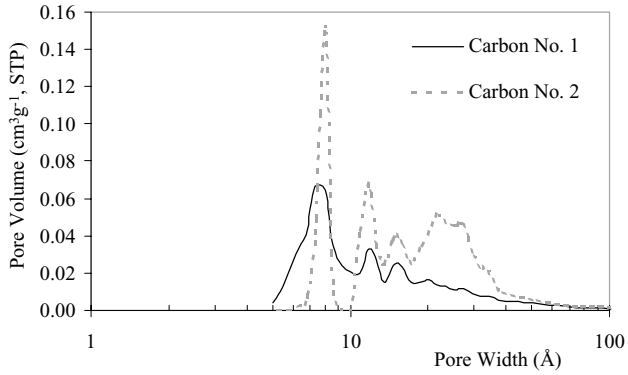

Fig. 1. Pore size distribution of carbon powders 1 and 2 according to the density functional theory.

Table 1
Pore characteristics of nanoporous carbon powders used for the preparation of electrodes

Parameter	Carbon no. 1	Carbon no. 2
BET surface area, S_a ($m^2\,g^{-1}$)	1449	1922
Micropore surface area, S_m ($m^2\,g^{-1}$)	1518	1749
Micropore volume, V_m ($cm^3\,g^{-1}$)	0.63	0.83
Total pore volume, V_{tot} ($cm^3\,g^{-1}$)	0.80	1.09
Median pore diameter[a], D_{HK} (Å)	6.8	9.4

[a] Median pore diameter according to Horvath–Kawazoe method.

thicknesses. The pore size distribution was calculated according to the density functional theory (DFT).

The electric double layer capacitors (EDLC) were assembled so that the positivly charged electrodes were made from the carbon no. 1 with a micropore predominantly below 10 Å and the negatively charged electrodes from the carbon no. 2 with a significant fraction of micropores between 10 and 30 Å. The electrodes were attached to current collector: Al foil, and interleaved with an ion-permeable separator paper from Codashi Nippon. The electrode pairs from positively and negatively charged electrodes with a visible surface area of 64.5 cm^2 were connected in parallel. The electrode pack prepared was placed in a sealed box, kept at 100 °C under vacuum for 3 days to remove all gases absorbed and then impregnated with electrolyte. Four EDLC cells were filled with different electrolytes comprising 1.0 M triethylmethylammonium tetrafluoroborate (TEMA) in anhydrous acetonitrile (AN, Riedel-de Haën, H_2O < 0.003%), anhydrous Selectipur® propylene carbonate (PC, Merck, H_2O < 0.003%), Selectipur® γ-butyrolactone (GBL, Merck, H_2O < 0.003%) and Selectipur® dimethyl ketone (DMK, Alfa, H_2O < 0.03%). TEMA salt (Stella) was dried under vacuum at 170 °C prior to preparing the electrolyte solution. The triethylmethylammonium tetrafluoroborate has been selected out because the solubility of this electrolyte is noticeable higher at lower temperatures in comparison with tetraethylammonium tetrafluoroborate and therefore the more higher conductivities for electrolyte at lower temperatures can be achieved. Selected physical characteristics of the solvents used in the EDLCs are presented in Table 2 [19].

2.1. Electrochemical study

The EDLCs were preconditioned by continuous cycling between 2.3 and 1.15 V with the current $I = 1$ A during 3 days prior performing the further electrochemical studies. It was observed that approximately 1000 cycles (that took about 24 h) were needed to stabilize the inner resistance and capacitance of AN based EDLC. The EDLCs based on PC, GBL and DMK electrolytes demonstrated stable characteristics of polarization after 2000 cycles (approximately 2 days). After preconditioning the pressure release valve was opened to remove the gases formed during continuous potential cycling.

2.2. The cyclic voltammetry (j, E) curves

The cyclic voltammetry curves for EDLCs, based on 1.0 M TEMA in AN, GBL, DMK and PC electrolyte are presented in Fig. 2. The EDLCs with the AN, GBL and PC electrolytes are ideally polarizable in the potential region from 0 to 3 V. The experimental data revealed that for all the EDLCs the *j*, *E*-curves are independent of the number of current cycles, *n*, if $n \geq 5$.

At higher potential scan rates, the well expressed distortion effects observed in the *j*, *E*-curves for GBL, DMK and PC are caused by the higher internal resistance of the EDLCs compared with the acetonitrile based electrolyte EDLCs, as well as by the onset of so-called "electrolyte starvation" effect, discussed by Conway and Pell [1,16] and associated with the withdrawal of the electrolyte ions from the pore bulk electrolyte due to the adsorption of ions on the double layer interfaces when they become charged.

In Fig. 3a and b, it is seen that the current responses expectedly increase with higher scan rate values. The voltammograms become distorted from the ideal rectangular form characteristic for an ideal capacitor demonstrating constant capacitance [1]. The corresponding capacitance behavior for EDLCs are shown in Fig. 3c, which indicates that the capacitor based on 1.0 M TEMA in acetonitrile (Fig. 3c) behaves as almost ideal EDLC already at scan rate of 50 mV s^{-1}. The GBL based capacitor behaves quite similarly to AN system, however the deviation from the rectangular shape at sweep rate of 50 mV s^{-1} is obvious. The capacitor modules consisting acetone and propylene carbonate electrolyte solutions (Fig. 3d) behave as ideal capacitors at scan rates below 10 mV s^{-1}. Furthermore, slightly increased capacitance in the module with acetone at cell potential values exceeding 2.0 V are indication of the more narrow electrochemical window (i.e. of the more narrow region of ideal polarizability) and probably indicates the beginning of the Faradaic reactions in the EDLC. The increased capacitance at higher

Table 2
The physical parameters of the solvents [19]

Solvent	Melting point (°C)	Boiling point (°C)	Viscosity (Pa s^{-1})	Dielectric constant (ε)	Density (kg m^{-3})
AN	−43.8	81.6	0.369	36.64	0.786
GBL	−43.3	204.0	1.72	39.0	1.128
PC	−48.8	241.7	2.513	66.14	1.205
DMK	−94.8	56.0	0.306	21.01	0.790

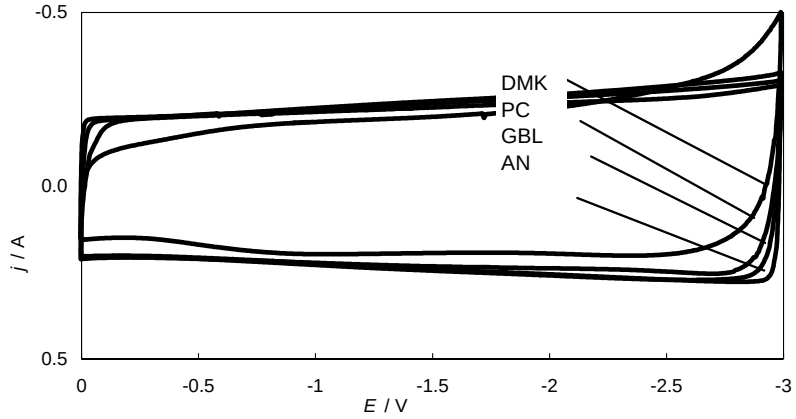

Fig. 2. The cyclic voltammetry curves at potential scan rate of 10 mV s^{-1} for the EDLCs in 1.0 M TEMA in AN, GBL, DMK and PC.

voltage is decrease of the effective size of electrolyte ions at increased voltage. This effect was recently observed and discussed for the skeleton carbon electrodes [2,3].

2.3. Galvanostatic cycling study of the cells

The EDLCs were tested at constant current charge/discharge regimes in voltage range from 1.15 to 2.3 V. The current was varied from 0.5 to 8.0 A. The discharge capacitance was calculated from the data of third cycle according to Eq. (10). Measurements were repeated at various fixed temperatures in the region $-30\,^{\circ}C < T < +60\,^{\circ}C$ to study the stability of EDLCs parameters. The internal resistance value was calculated from the IR—drop (at fixed dt = 10 ms) according to Eq. (11).

The shortest discharge cycle observed for EDLCs based on DMK, presented in Fig. 4, corresponds to the lowest capacitance value of EDLC modules studied. The similar effect is also observed at low current values (Fig. 5). It should be noted that the capacitance decreases almost proportion-

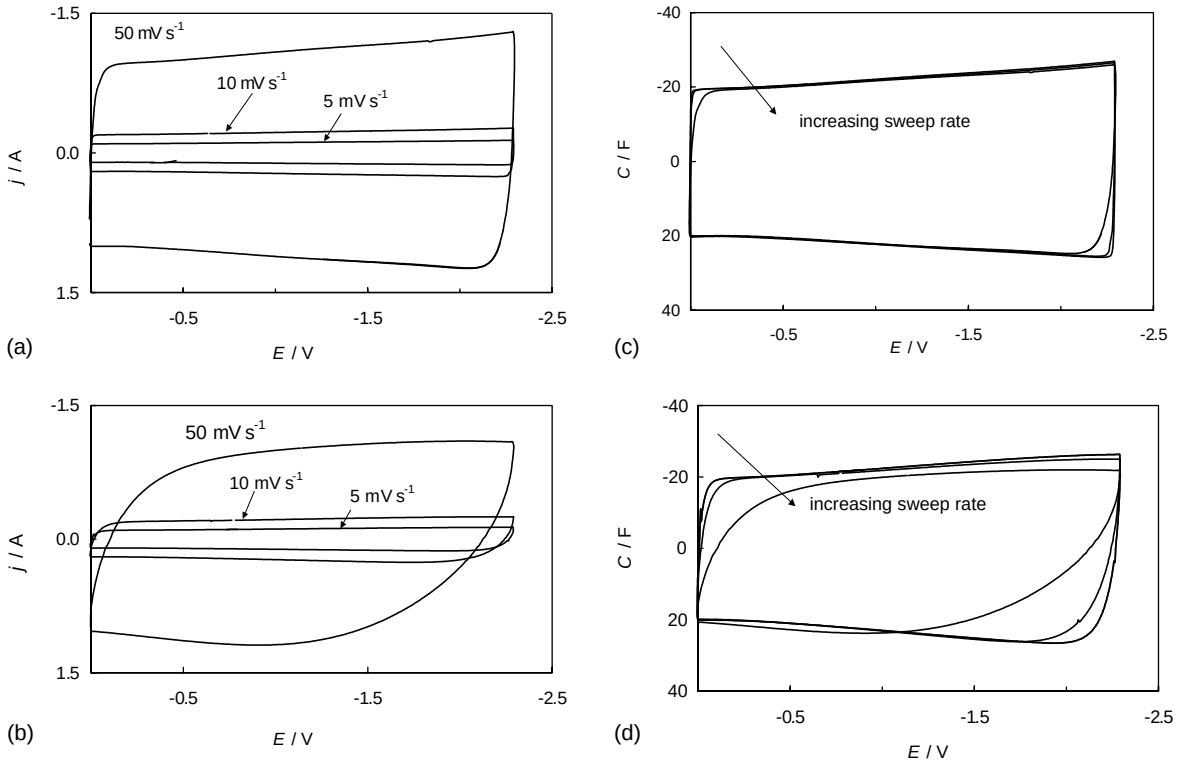

Fig. 3. Current density vs. capacitor potential curves for AN (a), and PC (b) electrolyte corresponding EDLC systems at potential scan rates of 50, 10 and 5 mV s^{-1} noted in figure. Respective C, E-curves (c, d) calculated from j, E-curves at potential scan rates of 50, 10 and 5 mV s^{-1}, noted in figure.

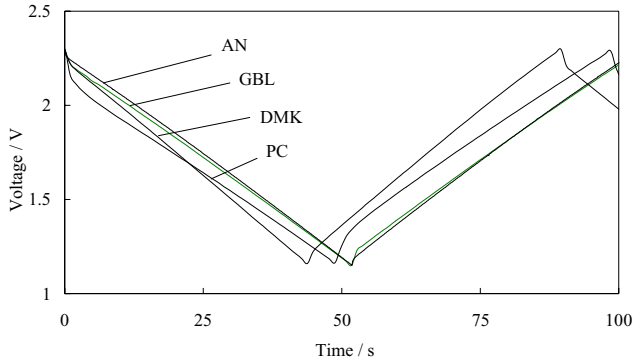

Fig. 4. Constant current charge/discharge cycle at $I = 0.5$ A and $T = 298$ K for the EDLCs filled with different electrolytes, noted in figure.

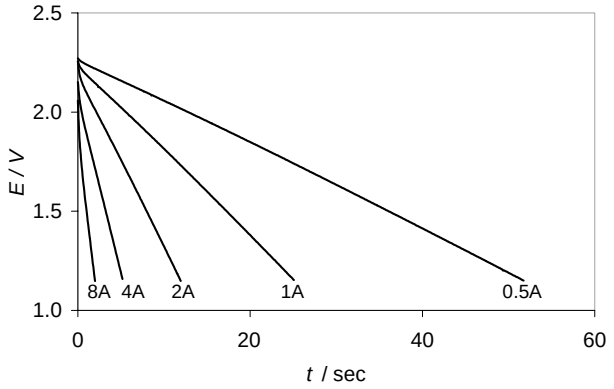

Fig. 5. Constant current discharge profiles measured for EDLC at $T = 298$ K filled with 1.0 M TEMA in AN at constant current densities, noted in figure.

ally with increasing the current with exception of PC based EDLC (Fig. 6). The dependence of C versus I increases with decreasing temperature and is also dependent on the electrolyte, particularly on viscosity of the solvent. The specific capacitance and resistance data are presented in Table 3.

The capacitance values presented in Table 3 decrease from AN to PC electrolyte at ambient temperatures. The temperature dependence is most significant for PC-based EDLC that

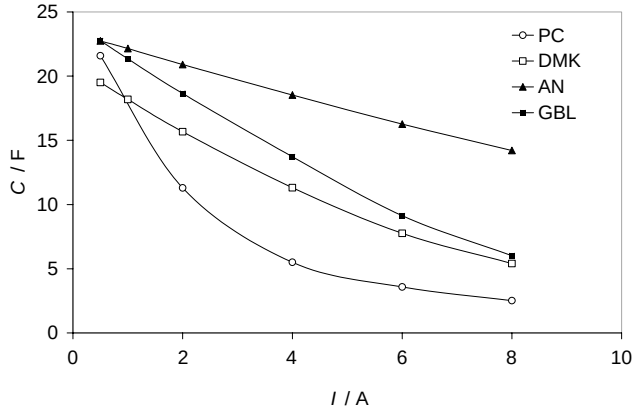

Fig. 6. Discharge capacitance vs. current density plots at $T = 298$ K for the EDLCs based on different nonaqueous electrolytes, noted in figure.

Table 3
The specific capacitance and resistance values for the EDLC cells

Solvent	Capacitance (F)			Resistance (Ω cm^2)		
	−30 °C	+20 °C	+60 °C	−30 °C	+20 °C	+60 °C
AN	22.4	22.7	22.9	1.0	0.6	0.5
GBL	19.8	21.6	22.7	3.0	1.2	1.0
DMK	17.6	21.0	21.7	4.5	1.2	1.3
PC	6.1	19.7	21.5	7.9	1.8	1.2

The capacitance for the cells is calculated according to Eq. (10) and the resistance per visible electrode surface area according to Eq. (11).

is also well supported by the highest viscosity among the solvents studied. Consequently the logical result was the almost stable capacitance and resistance over the temperature range from −30 to +60 °C for the EDLC comprising acetonitrile as the low-viscosity solvent. The specific resistance value (in Ω cm^2) is influenced by the choice of EDLC materials (i.e. carbon, separator, current outlet, etc.) and design of the EDLC cell. As a rule, the smaller is the capacitance value, the lower are the specific series resistance obtained. In present work, all cells had the same design, therefore the resistance values should be mainly influenced by the properties of the electrolyte and carbon. However, according to the systematic analysis of experimental results, the resistance values correlate well with the electrolyte molar conductivity values.

The cycling efficiency, so-called round trip efficiency (RTE) can be calculated as the ratio of capacitances measured during discharging and charging of EDLC, i.e. RTE = C(discharge)/C(charge), where the discharge and charge capacitance values are calculated according to Eq. (10).

Among capacitors studied, the round trip efficiency is the highest in acetonitrile-based EDLC and the RTE value decreases in the order of solvents AN > GBL > DMK > PC (Table 4). RTE is also influenced by temperature: the lower is the temperature, the lower is RTE. EDLC with acetone-based electrolyte has a RTE maximum at ambient temperature that could serve as indication of increased irreversibility of the processes in DMK based EDLC at elevated temperature. RTE value generally decreases when the current density is increased, but with exception of DMK. Although the latter phenomenon of acetone-based electrolyte is not clear yet, it could be caused by the worse cycleability of ketone type solvents in the wide region of electrode polarization.

Table 4
Round trip efficiency (RTE) for EDLC cells with different electrolytes measured at variable temperature and current density ($I = 0.5$ and 2.0 A)

Solvent	RTE (%) at $I = 0.5$ A			RTE (%) at $I = 2.0$ A		
	−30 °C	20 °C	+60 °C	−30 °C	20 °C	+60 °C
AN	95.9	97.6	97.9	87.4	93.2	94.9
GBL	86.1	93.9	96.3	70.9	86.4	90.7
DMK	83.1	92.2	80.6	68.9	85.6	83.9
PC	73.5	90.2	93.1	63.6	76.5	82.1

Table 5
Capacitance in farads of the EDLC calculated using data of different testing methods

Solvent	Measurements procedure for capacitance (F)		
	CV ($v = 10\,\text{mV s}^{-1}$)	CC ($I = 0.5\,\text{A}$)	EIS at $f = 10\,\text{mHz}$ (DC = 2.3 V, AC = 5 mV)
AN	22.9	22.7	25.6
GBL	23.1	22.8	26.0
PC	21.9	21.6	22.8
DMK	20.4	19.5	23.9

According to the data in Table 5, the capacitance values of the EDLC cells depend of the measurement technique used. The DC-capacitance values obtained from CC or CV measurements are almost similar, but substantially different from those calculated from the impedance data. In all cases the impedance spectrum yields the higher series capacitance C_s values for charged EDLCs. The exceptional case is the PC-based EDLC, which yields the lower C_s values—probably because the used frequency 10 mHz is still too high to establish the equilibrium C_s capacitance value in the high-viscosity PC electrolyte.

2.4. Electrochemical impedance study

From the Z'', Z' plots (Fig. 7) it can be found that all the capacitors behave as typical capacitors over the frequency range from 100 Hz to 10 mHz. The curve in figure can be divided into three main sections. At high ac penetrability (at low frequency $f \leq 0.1$ Hz) the carbon material behaves like porous material and the ac signal detects the large amount of the pore volume. This region of Z'', Z' plot is called a planar section and the phase-angle approaches asymptotically to $-80 \cdots -90^\circ$.

The second section lies in the region $10\,\text{Hz} < f < 0.1\,\text{Hz}$, where ac signal detects the less porous material and the curve slope on Cole–Cole or complex plane plots (Fig. 7) is almost 45°. The characteristics of plateau with the 45° slope depend on many factors including carbon properties, electrode thickness, separator and electrolyte characteristics, temperature, etc. EDLC cells under this study differed from each other only by the choice of the solvent. Therefore, the differences observed in the "45°-slope" region characteristics are mainly caused by the different properties of the electrolyte solution and may particularly be contributed with the electrolyte (solvent) viscosity. In the high-frequency region of ac the porous electrode behaves like a flat surface and therefore the capacitance obtained is by many orders of magnitude lower compared to the equilibrium capacitance at $\omega \to 0$. This region of Z'', Z'-plots (usually at $f = 100$ Hz) is used to determine the series resistance of the double-layer capacitor, $Z'_{(\omega \to 0)} = R_{\text{int.}}$. The resistance component observed at $Z'' = 0$ in Fig. 7 satisfactorily matches the electrolyte conductivity and resistance values presented in Tables 3 and 6.

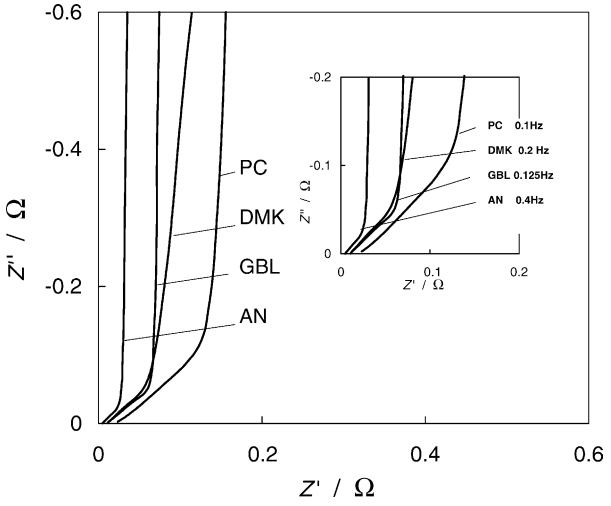

Fig. 7. Nyquist plots for the EDLC based on different solvents, noted in figure.

Based on the data in Table 6 it was concluded that the specific capacitance (F cm^{-2}) is weakly influenced by the choice of the solvent in electrolyte composition as long as the same concentration of electrolyte salt is considered. In the case of propylene carbonate the somewhat lower C_s value is probably due to the high viscosity of PC that does not allow reaching the limiting capacitance at relatively high frequency ($f = 10$ mHz). The data in Tables 1 and 6 well confirm the influence of electrolyte molar conductivity on the so-called pore resistance and electrolyte resistance values. The volumetric capacitance of the carbon electrodes has almost similar value in all EDLC cells tested in this study. Our investigations reveal the clear advantage of acetonitrile based capacitor, particularly due to the low total impedance.

Relationships between series resistance and series capacitance versus frequency are presented in Fig. 8 and well support the data demonstrated in Table 6. In Fig. 8, it is also seen that all test cells have a plateau on the C_s-curve at very low ac frequency that is characteristic of the EDL formation in fine micropores.

Fig. 9 shows the phase angle versus frequency relationship for all electrolyte compositions under study, however the ideal behavior of the capacitor according to the phase angle is not reached in any electrolyte studied. Perhaps the closest to the ideal one is the cell based on AN with the phase angle value of $\delta \approx -90^\circ$, which indicates the nearly pure capacitive behavior of EDLC at low frequencies. The cells filled with GBL and DMK electrolytes have slightly lower absolute phase angle values compared to the AN electrolyte, which may be caused by the specific interactions between solvent bearing carbonyl group and nanoporous carbon [1]. The same dependence seems to be true for the PC, however the much lower phase angle value measured at constant frequency indicates the existence of the additional limiting factors, one of which could be the low molar conductivity of PC electrolyte.

Table 6
Electrochemical parameters of the EDLC cells calculated from electrochemical impedance spectroscopy data at 2.3 V (DC)

Solvent	C_s (F cm^{-2})	R_{el} (Ω cm^2)	R_{pore} (Ω cm^2)	R_s at $f = 100$ Hz (Ω cm^2)	Average capacitance of carbon electrodes	
					(F g^{-1})	(F cm^{-3})
AN	0.40	0.29	1.20	0.31	106	71
GBL	0.40	0.65	2.79	0.75	106	69
DMK	0.37	0.70	3.91	0.77	102	70
PC	0.35	1.37	4.94	1.67	94	65

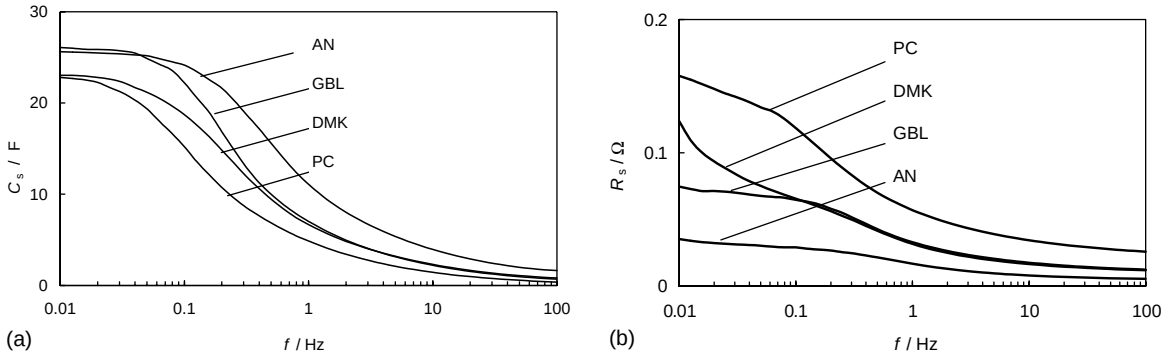

Fig. 8. Series resistance and series capacitance of the cells based on different solvents, noted in figure.

Table 7
Energy and power performance of the EDLC cells, calculated from galvanostatic cycling test data at the discharge potentials up 2.3–1.15 V

Solvent	Usable energy (Wh dm^{-3})	R_s (Ω cm^2)	Power density[a] (90% eff) (W cm^{-3})	Real max. power[b] (W cm^{-3})	Matched power[c] (W cm^{-3})
AN	5.5	0.63	6.3	15.5	59.6
GBL	5.5	1.18	3.6	6.5	31.8
DMK	5.4	1.21	3.6	6.5	32.1
PC	4.5	1.81	2.2	2.6	19.5

[a] Power density at 90% efficiency according to Eqs. (14) and (16).
[b] Real maximum power obtained from Ragone plot (Fig. 10) when $E \rightarrow 0$.
[c] Matched power according to Eq. (15).

2.5. Constant power (CP) study

Fig. 10 presents the Ragone plot, i.e. the energy and power relationship of the unpacked capacitors that is derived from CP curves. Here, the unpacked capacitor is defined as the EDLC cell without case. More precisely, it includes the volume and weight of terminals, carbon electrodes, separator and electrolyte solution.

The volumetric energy densities at moderately low power density were rather similar in all capacitors. This is in a good accordance with the capacitance values obtained from constant current (CC) study. The behaviour of capacitor filled with acetonitrile retains almost constant energy in the wide

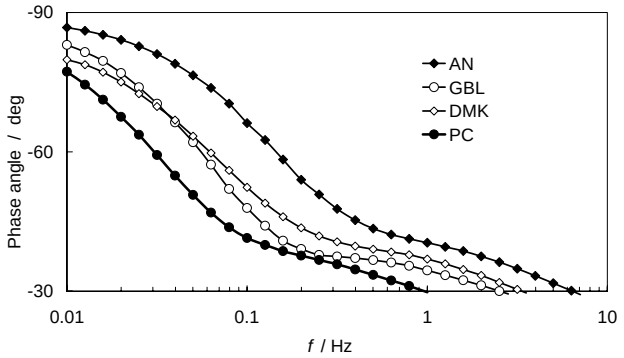

Fig. 9. The plot of phase angle vs. frequency for EDLC cells with different solvents, noted in figure.

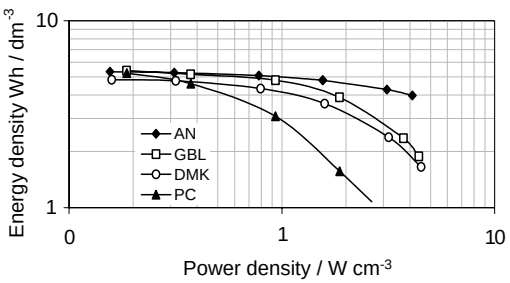

Fig. 10. Ragone plot for the unpacked EDLC cells with different electrolyte solutions, measured at +20 °C.

range of studied power. The capacitors filled with acetone and γ-butyrolactone electrolytes behave rather similarly: the significant energy decrease at higher power values was observed. Similar behavior of these two electrolytes was also seen in other figures (Figs. 6–9). The behaviour of capacitor filled with propylene carbonate was significantly different from other studied cells—it had noticeable energy/power dependence already at rather low power values.

The maximum power values (at $E = 0$) calculated from the Ragone plots and presented in Table 7 well agree with the internal resistance values of capacitors (cf. data in Tables 3 and 6). Power density values in Table 7 calculated according to Eqs. (14) and (16) match with the experimental values measured at RTE 90%.

3. Conclusions

The electrical double layer capacitor (EDLC) cells comprising nanoporous carbon electrodes and different electrolyte solutions—1.0 M triethylmethylammonium tetrafluoroborate in acetonitrile (AN), γ-butyrolactone (γ-BL), acetone (DMK) and propylene carbonate (PC)—were thoroughly studied using several electrochemical testing procedures and techniques. It was found that most of important parameters such as the series capacitance, series resistance and phase angle noticeably depend on the electrolyte composition as well as on the cell potential applied. It was established that the so-called pore resistance, i.e. internal distribution of the electrode resistance rises in the following sequence of solvent: AN < GBL < DMK < PC. It was shown that the value of characteristic frequency depends on the electrolyte solution and on the electrode potential, i.e. on the nature and structure of solvated ions adsorbed at the surface of the nanoporous carbon electrode. It should be noted that the results of the galvanostatic tests and estimated Ragone plots show the clear advantage of the acetonitrile-based electrolytes in carbon/carbon EDLCs.

Acknowledgements

This work was supported by Skeleton Technologies and in part by the Estonian Science Foundation under project 4568.

References

[1] B.E. Conway, Electrochemical Supercapacitors. Scientific Fundamentals and Technological Applications, Kluwer Academic Publishers/Plenum, New York, 1999.
[2] E. Lust, G. Nurk, A. Jänes, M. Arulepp, L. Permann, P. Nigu, P. Möller, Condens. Mat. Phys. 5 (2002) 307.
[3] E. Lust, N. Nurk, A. Jänes, M. Arulepp, P. Nigu, P. Möller, S. Kallip, V. Sammelselg, J. Solid State Electrochem. 7 (2003) 91.
[4] United States Patent Application Publication No. 2002/0097549, 2002.
[5] G. Salitra, A. Soffer, L. Eliad, Y. Cohen, D. Aurbach, J. Electrochem. Soc. 146 (2000) 2486.
[6] J.R. Macdonald, Impedance Spectroscopy, Wiley, New York, 1987.
[7] I. Roušar, K. Micka, A. Kimla, Electrochemical Engineering, vol. 2, Elsevier, Amsterdam, 1986.
[8] R. de Levie, J. Electroanal. Chem. 281 (1990) 1.
[9] G. Paasch, K. Micka, P. Gersdorf, Electrochim. Acta 38 (1993) 2653.
[10] R. de Levie, Electrochim. Acta 8 (1963) 751.
[11] R. de Levie, Electrochim. Acta 8 (1964) 1231.
[12] H. Keiser, K.D. Beccu, M.A. Gutjahr, Electrochim. Acta 21 (1976) 539.
[13] M. Arulepp, A. Jänes, G. Nurk, L. Permann, P. Nigu, E. Lust, in: Abstracts of the 51st Annual ISE Meeting, Warsaw, Poland, 2002, p. 946.
[14] G. Nurk, A. Jänes, M. Arulepp, P. Nigu, L. Permann, E. Lust, in: Abstracts of the Joint International Meeting of ISE and ECS, abstr. 1006, San Francisco, 2001.
[15] D. Qu, H. Shi, J. Power Sources 74 (1998) 99.
[16] W.G. Pell, B.E. Conway, J. Electroanal. Chem. 500 (2001) 121.
[17] H.-K. Song, Y.-H. Jung, R.-H. Lee, L.H. Dao, Electrochim. Acta 44 (1999) 3513.
[18] J. Leis, A. Perkson, M. Arulepp, P. Nigu, G. Svensson, Carbon 40 (2002) 1559.
[19] R.L. David, H.P.R. Frederisce (Eds.), CRC Handbook of Chemistry and Physics, 76th ed., CRC Press, New York, 1995.